The effect of event consistent smoothing on CRS imaging

T. Klüver

email: *Tilman.Kluever@gpi.uni-karlsruhe.de*
keywords: *CRS stack,wavefield attributes,smoothing*

ABSTRACT

The kinematic wavefield attributes, extracted automatically from seismic prestack data by means of the Common-Reflection-Surface stack, have found several applications. However, the attributes determined by means of coherence analysis are subject to fluctuations due to noise in the prestack data as well as to outliers due to a failure of the splitted search stragey used in the CRS method. These problems can be overcome partially by the application of an event-consistent smoothing algorithm. In this paper, I review the algorithm for the 2D case and give its extension to the 3D case. The effect of event-consistent smoothing on CRS imaging will be demonstrated using a small 2D real data example.

INTRODUCTION

The CRS stack has been developed as an alternative stacking procedure to the conventional chain of normal-moveout (NMO) correction/dip-moveout (DMO) correction and stack. The determined CRS attributes have found several applications, e.g. the determination of a velocity macromodel for depth imaging. All these applications suffer from fluctuations of the attributes due to noise in the prestack data as well as insufficiences in the search strategy. To overcome this problems partially Mann and Duveneck (2003) introduced an event-consistent smoothing algorithm. In this paper I give a rewiev of their work and describe the extension to the 3D case. Finally, I investigate more detailed the influence of event-consistent smoothing on CRS imaging using a 2D real data example.

EVENT CONSISTENT SMOOTHING

The implementation of the event consistent smoothing algorithm follows the description which was given by Mann and Duveneck (2003). I will describe it here in a manner also valid for the 3D case which has been implemented meanwhile.

In order to perform an event-consistent smoothing of kinematic wavefield attributes, the smoothing window (2D case) or volume (3D-case) has to be aligned with the reflection event in the ZO section/volume and the reliability of the associated wavefield attributes has to be considered. The CRS wavefield attributes α and β give the emergence angle and azimuthal direction of the normal ray for the ZO sample under consideration. Using these two angles and the near-surface velocity v_0 used in the CRS stack the slowness vector $\mathbf{p}$ of the local segment of the Normal-incidence-point(NIP)- and Normal(N)-wavefront can be calculated which is connected to the orientation of the event in the ZO section/volume. The slowness vector is given by

$$\mathbf{p} = \frac{1}{v_0} \left(\cos\alpha \sin\beta, \sin\alpha \sin\beta, \cos\beta\right)^T \tag{1}$$

The slowness vector $\mathbf{p}$ itself is independent of the near-surface velocity. This means, that the smoothing is performed correctly even if a wrong velocity was used in the CRS stack. The reliability of the attributes for a ZO sample is given by the coherence value obtained along the corresponding stacking operator in the prestack data. In order to take into account only reliable information, ZO samples with a coherence value

S below a user-defined threshold S_{min} should not contribute to the smoothing. According to Mann and Duveneck (2003) such low coherence values occur due to several reasons:

- The ZO sample under consideration is not located on a locally coherent event. In this case the obtained attribute values are meaningless as no coherent energy contributes to the stack.

- Due to a low signal-to-noise ratio in the prestack data the wavefield attributes are subject to fluctuations. These fluctuations are not supported by the theory. As long as we are dealing with situations where zero-order ray theory is valid the attributes can vary only smoothly along the reflection event. Along the seismic wavelet, the attributes should be virtually constant (Mann and Höcht, 2003).

- The splitted search strategy fails to detect the global coherence maximum or the global coherence maximum does not correspond to the same reflection event as the maximum of neighbouring samples. This leads to localized outliers in the attribute sections.

- The prestack data contain strongly non-hyperbolic events. In this case the aperture choice for the CRS stack should be reconsidered.

To take conflicting dip situations into account, neighbouring samples are only included in the smoothing process if the normal vector to the reflection event, calculated from the attributes of this sample, encloses an angle below an user-defined threshold $\Delta\gamma_{max}$ with the corresponding normal vector calculated from the attributes of the sample to be smoothed. This is the natural extension to the 3D case of the original description given by Mann and Duveneck (2003) for the 2D case.

DATA EXAMPLE

In this section I show the effect of the smoothing on the CRS results using a small part of a 2D real dataset. First, the CRS stack including optimization was performed. Then, the attributes used for the initial stack were smoothed. Using these smoothed attribute values, the initial stack and optimization were performed once again. The obtained stack and attribute sections are shown from Figure (1) to Figure (5).

First a closer look to the final stack sections (Figure (1)). Comparing the initial stack with the optimized stack (Figures (1(a)) and (1(b))), both obtained using unsmoothed attributes, one can clearly see the increased reflector continuity on some relatively weak events. Also the right end of the strong reflection event in the center of the section is improved regarding continuity. At least the same improvement can be gained by smoothing of the used attributes. The initial stack section using smoothed attributes is shown in Figure (1(c)). A subsequent optimization shows no visible improvement in the stack result (Figure (1(d))).

These observations are supported considering the corresponding coherence sections (Figure (2)). Comparing the coherence obtained using unsmoothed initial attributes, shown in Figure (2(a)), with the corresponding section obtained with smoothed attributes (Figure (2(c))), one can clearly see the improved lateral continuity. In both cases, continuity is increased performing an optimization. The optimized results for unsmoothed and smoothed attributes show nearly identical coherence. Performing the optimization after smoothing closes some gaps. That means low coherence samples, which are due to a failure of the splitted search strategy, are removed. This removal can't be obtained just by optimization of the unsmoothed attributes which is obvious comparing Figure (2(b)) with Figure (2(d)). This means, in cases where the CMP-search fails and its result is far from the searched for global maximum, this maximum might not be found even by simultaneous optimization of all three attributes.

These observations can also be made in the attribute sections of the NIP-wave radius R_{NIP} (Figure (4)), of the Normal-wave radius R_N (Figure (5)), and of the emergence angle α (Figure (3)). Both, optimization and smoothing of the initial attributes, remove sharp edges in the attribute values inside of events. However, optimization, either before or after smoothing, leads to some fluctuations. This effect is especially visible in the sections of R_N in Figure (5). Surprisingly, the optimization after smoothing yields nearly the same attribute values than the optimization before smoothing. This is different, especially for R_{NIP}, where smoothing before optimization yields higher lateral continuity in the attribute values as it is expected from theory.

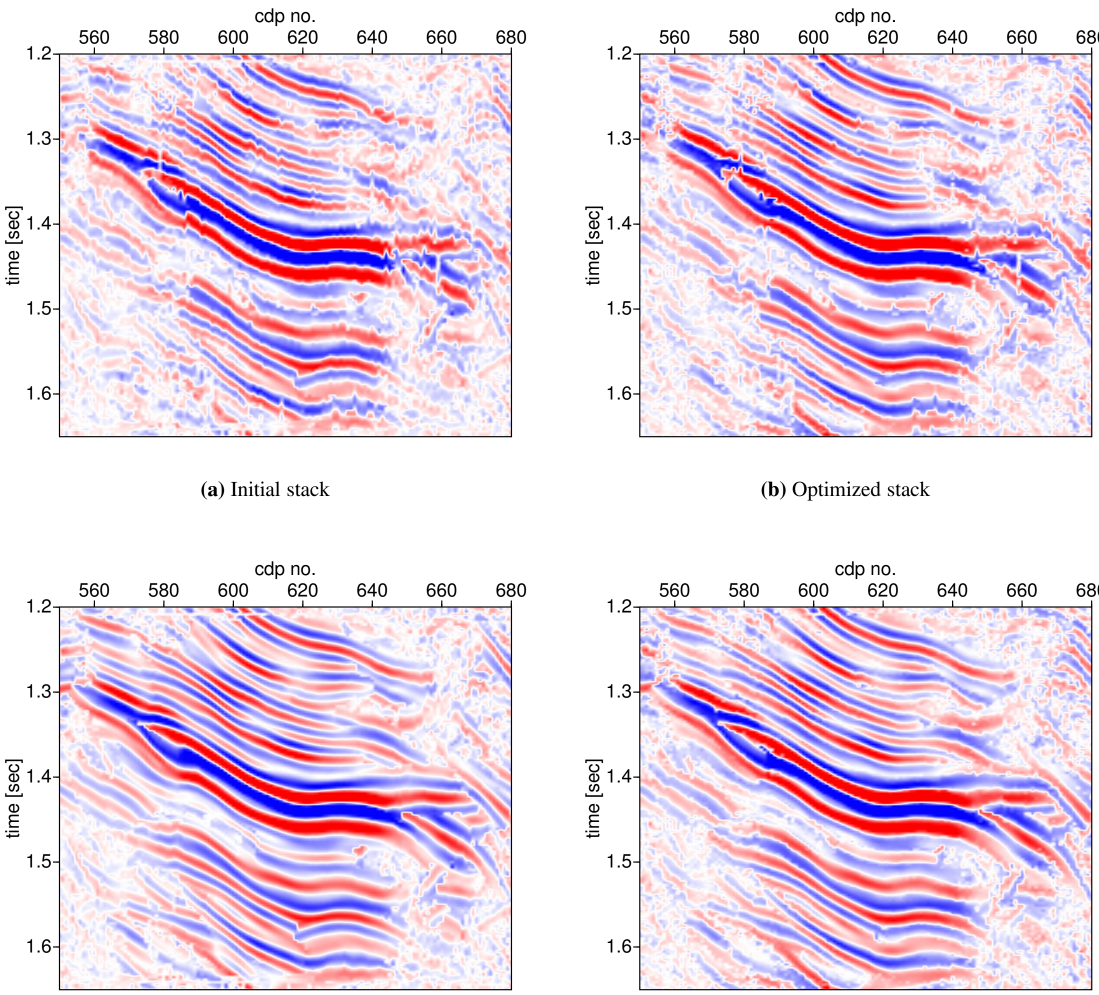

(a) Initial stack

(b) Optimized stack

(c) Initial stack with smoothed attributes

(d) Optimized stack with smoothed attributes

Figure 1: Initial and optimized tack results using unsmoothed and smoothed attributes

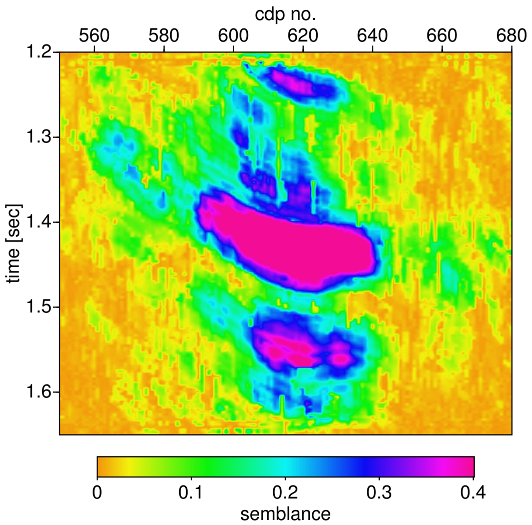

(a) Initial coherence

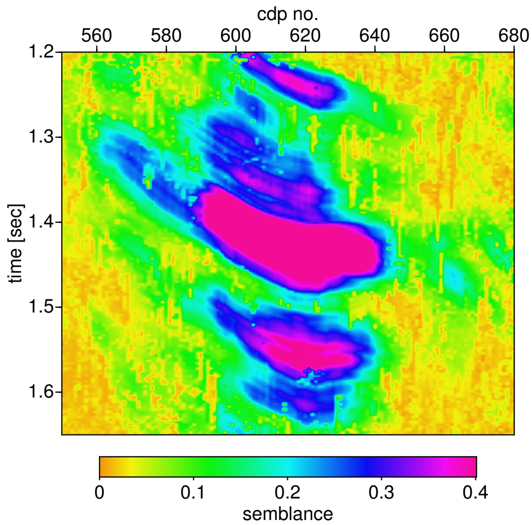

(b) Coherence after optimization

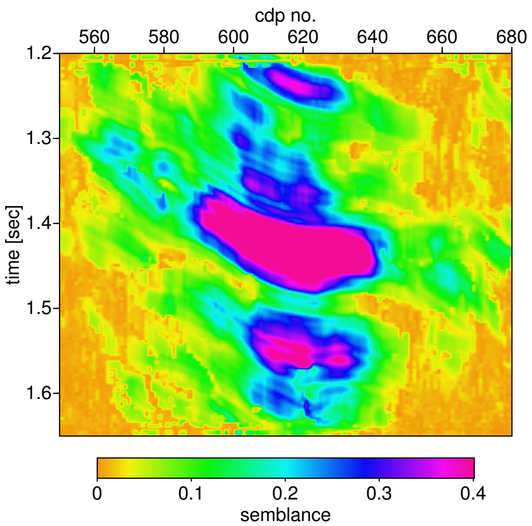

(c) Initial coherence with smoothed attributes

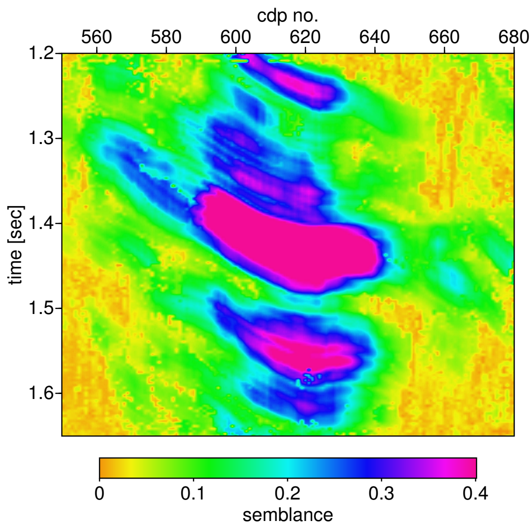

(d) Coherence after optimization with smoothed attributes

Figure 2: Initial and optimized coherence using unsmoothed and smoothed attributes

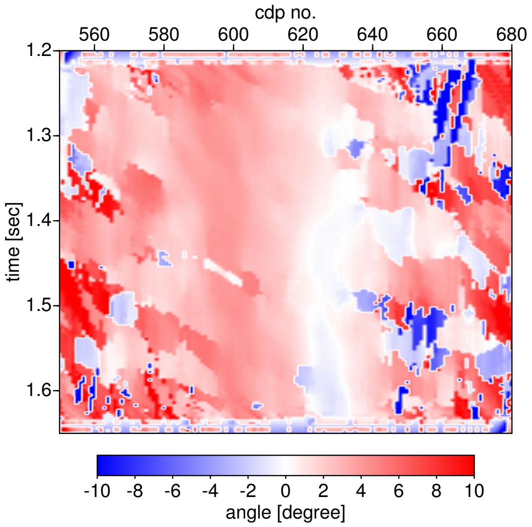

(a) Initial angle

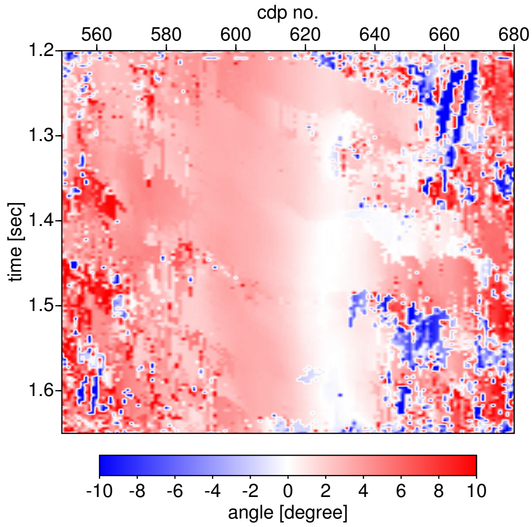

(b) Optimized angle

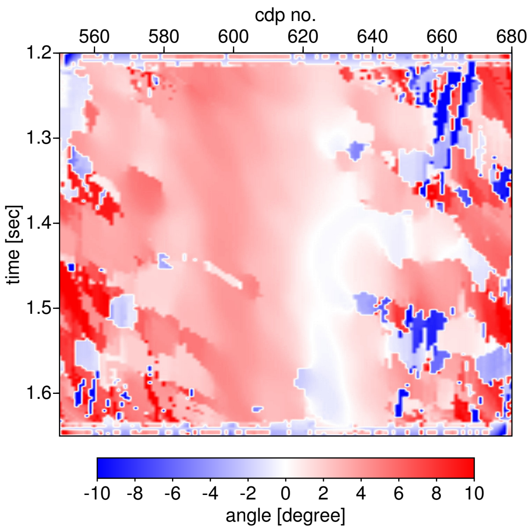

(c) Smoothed initial angle

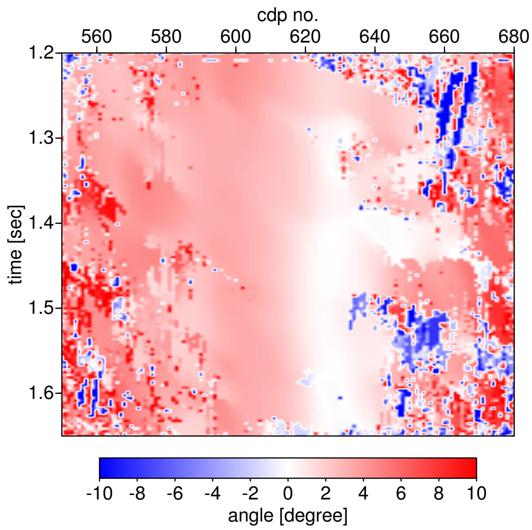

(d) Smoothed optimized angle

Figure 3: Initial and optimized angles before and after smoothing

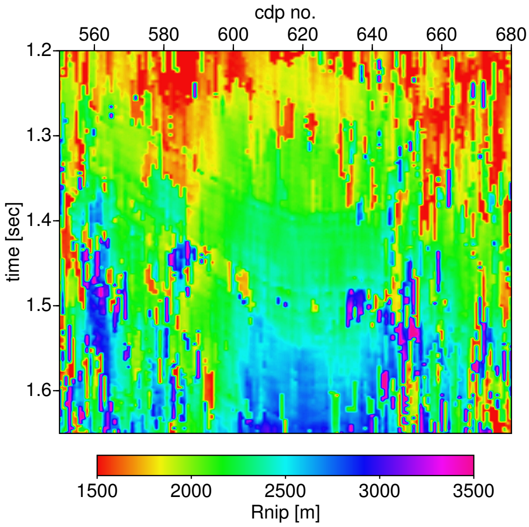

(a) Initial NIP wave radius

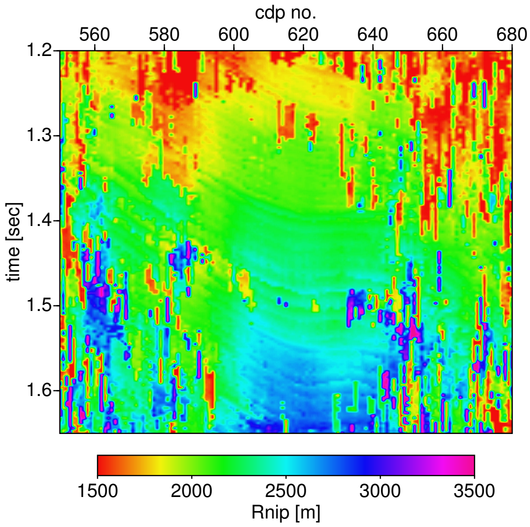

(b) Optimized NIP wave radius

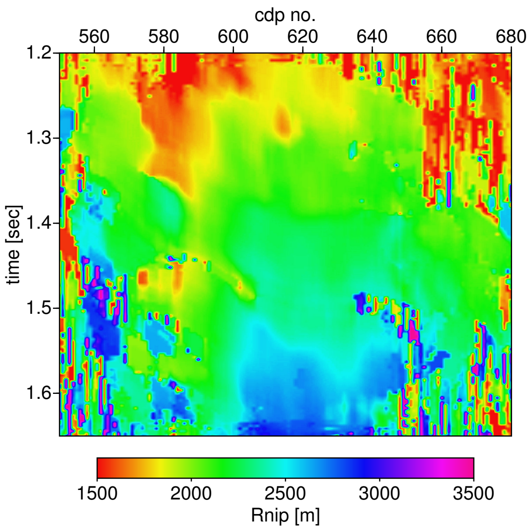

(c) Smoothed initial NIP wave radius

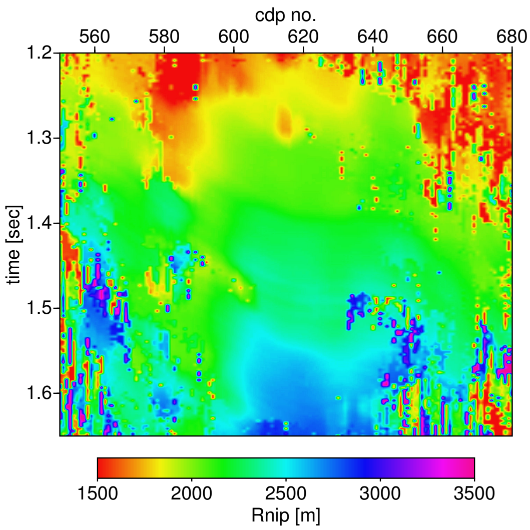

(d) Smoothed optimized NIP wave radius

Figure 4: Initial and optimized NIP wave radii before and after smoothing

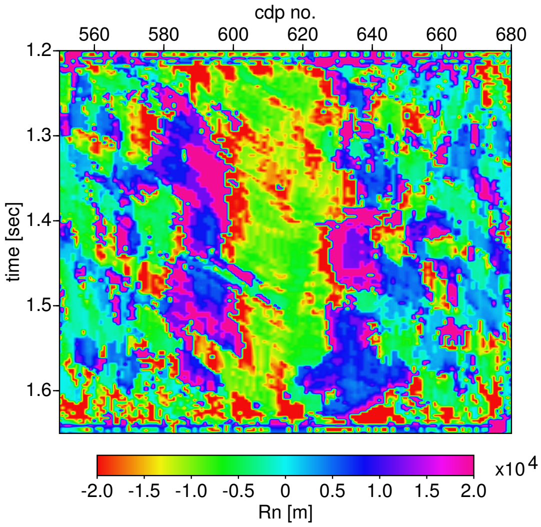

(a) Initial Normal wave radius

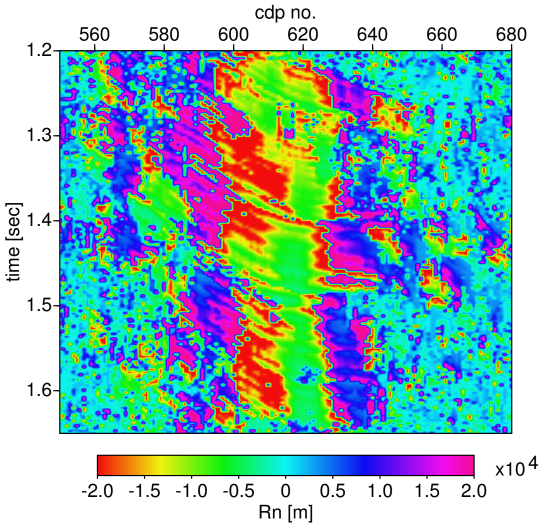

(b) Optimized Normal wave radius

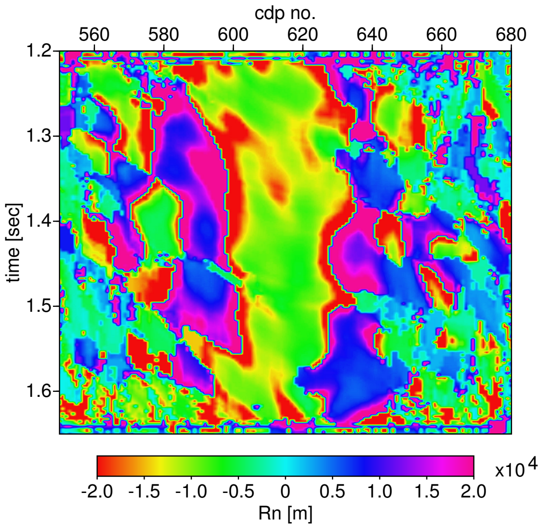

(c) Smoothed initial Normal wave radius

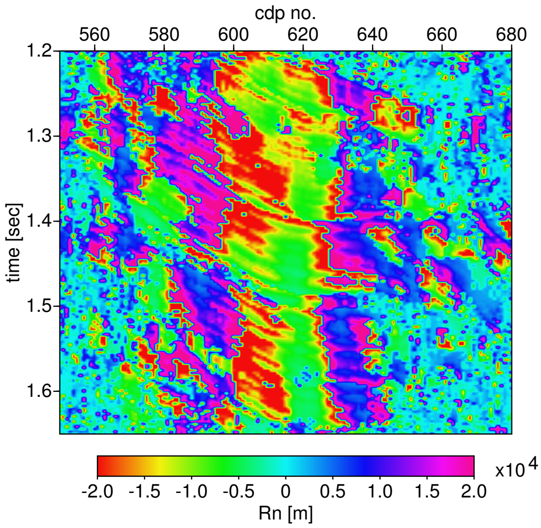

(d) Smoothed optimized Normal wave radius

Figure 5: Initial and optimized Normal wave radii before and after smoothing

CONCLUSIONS

The application of event-consistent smoothing can clearly improve CRS imaging. Especially, the quality of the obtained attributes for further applications is improved. The example shown in the previous section demonstrates that in the case the initial CMP search fails for some reason the optimal attribute triplet might not be found even by a simultaneous optimization. This clearly indicates the weakness of a splitted search strategy. Event-consistent smoothing can circumvent this problem partially. It would be interesting to see, how a simultaneous search for all attributes behaves. However, such a search is computationally very expensive. If event-consistent smoothing gives results comparable to a simultaneous search it is clearly the faster way of improving the quality of CRS imaging and especially of the obtained attributes.

ACKNOWLEDGMENTS

This work was kindly supported by the sponsors of the *Wave Inversion Technology (WIT) Consortium*, Karlsruhe, Germany.

REFERENCES

Mann, J. and Duveneck, D. (2003). Short note: event-consistent smoothing of kinematic wavefield attributes for stacking and inversion. *Annual Report, Wave Inversion Technology Consortium*, pages 75–81.

Mann, J. and Höcht, G. (2003). Pulse stretch effects in the context of data-driven imaging methods. In *65th Mtg. Eur. Assn. Geosci. Eng., Extended Abstracts,* Session P007.